Recent ab initio phase diagram studies: Iridium

IOP Conf. Series: Journal of Physics: Conf. Series **950** (2017) 042021 doi:10.1088/1742-6596/950/4/042021

Recent ab initio phase diagram studies: Iridium

L Burakovsky[1], M J Cawkwell[1], D L Preston[2], D Errandonea[3] and S I Simak[4]

[1] Theoretical and [2] Computational Physics Divisions, Los Alamos National Laboratory, Los Alamos, New Mexico 87545. USA
[3] Departamento de Física Aplicada-ICMUV, MALTA Consolider Team, Universidad de Valencia, Edificio de Investigación, C/Dr. Moliner 50, Burjassot, 46100 Valencia, Spain
[4] Department of Physics, Chemistry and Biology, Linköping University, 58183 Linköping, Sweden

E-mail: burakov@lanl.gov

Abstract. The phase diagram of iridium is investigated using the Z methodology in conjunction with the VASP *ab initio* molecular dynamics package. The Z methodology is a novel technique for phase diagram studies which combines the direct Z method for the computation of melting curves and the inverse Z method for the calculation of solid-solid phase boundaries. We compare our results to the available experimental data on iridium. We offer explanation for the 14-layer hexagonal structure observed in experiments by Cerenius and Dubrovinsky.

1. Introduction

Iridium (Ir) is one of the very special materials in nature. It is the only refractory face-centered cubic (fcc) metal with a melting point of 2719 K [1]. Its shear modulus, $G = 210$ GPa [2], is the largest among such fcc metals, and the second largest among all the elemental metals behind hexagonal close-packed (hcp) metal osmium (Os) with $G = 222$ GPa [2]. Ir is also one of the two most dense elemental metals having a density of 22.65 g/cc at ambient pressure (P) and T=0 or 22.56 g/cc at T=293.15 K [1] along with Os for which the corresponding values are essentially the same: 22.66 and 22.59 [3]. Because it exhibits excellent mechanical properties and high resistance to oxidation and corrosion at elevated T, Ir is used in numerous applications as a static component at high T and/or in aggressive environments. Despite the technological advances, the current understanding of the mechanical properties of Ir is rather poor, and the knowledge of its phase diagram is virtually nonexistent.

The similarity of the mechanical properties of Ir to those of the refractory hcp metals, specifically Os, and the fact that in a number of binary systems Ir forms solid solutions with a hcp structure which are stable in a wide range of concentrations, raised the issue of a potential phase transformation of Ir into the hcp structure. Such a fcc-hcp phase transformation in Ir was found in [4], and the transition P at room T was estimated to be 9 GPa and the fcc-hcp phase boundary was predictied to be a straight line with a positive slope of 150 K/GPa.

The subsequent experimental studies could not confirm a fcc-hcp transition in Ir at room T (except perhaps for a study by Cerenius and Dubrovinsky [5] discussed in what follows). It was however noted in [6] that the earlier data on the shock Hugoniot of Ir suggest the existence of a structural transformation above 1.14 Mbar. With the more recent shock Hugoniot data

available in the online Shock Wave Database (SWD) [7], it is now possible to firmly establish the existence of a solid-solid transformation on the Ir Hugoniot. Figure 1 shows two parallel segments shifted from each other by ~ 0.25 km/s that describe U_s-U_p shock Hugoniot data on Ir. This situation is typical of a solid-solid phase transition on the Hugoniot; for instance, figure 3 of ref. [8] demonstrates α-ω-β transition sequence in zirconium described by 3 parallel segments shifted from each other by ~ 0.2 and ~ 0.3 km/s, respectively [8]. The transition in Ir occurs at $1.10 < U_p < 1.36$ km/s or, if converted from U_s-U_p to P-U_p, at $140 < P < 180$ GPa [7], so we take the transition P to be 160 ± 20 GPa.

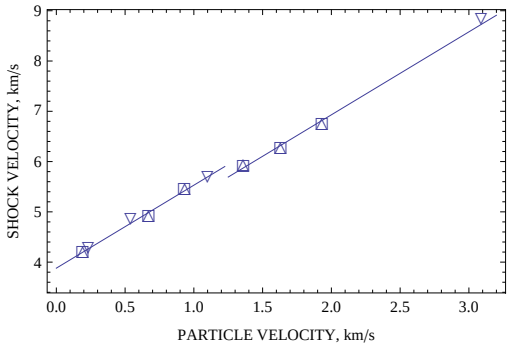

Figure 1. Shock velocity, U_s, vs. particle velovity, U_p, along the principal Hugoniot in Ir; data from [7]. A solid-solid phase transition occurs at $1.10 < U_p < 1.36$ km/s.

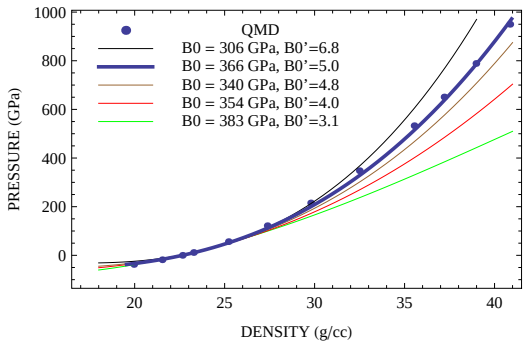

Figure 2. The T=0 Ir EOS from VASP compared to the experimental and theoretical 300 K Birch-Murnaghan EOSs.

In relatively recent experimental studies of Ir by Cerenius and Dubrovinsky [5], an unusual transition from fcc to a 14-layer hexagonal (hex) supercell was detected, at ~ 60 GPa. X-ray diffraction spectra showed a substantial increase in the intensity of the (111) peak of Ir accompanied by the appearance of a distinct saw-tooth pattern. Despite their low intensity, sufficient signal-to-noise ratio made it possible to resolve the peaks. Cerenius and Dubrovinsky noted that these peaks could not be explained by the formation of stacking faults or other types of defects (e.g., twinning) but could rather correspond to a distortion of the fcc lattice of Ir and the formation of a superlattice structure. These peaks were properly indexed and associated with a 14-layer hex supercell with cell parameters $a = 2.60$ Å and $c = 29.7$ Å at 65 GPa. Hence, the supercell is ideal to within 0.1%: $c/a = 29.7/2.60 = 11.423$ vs. $14\sqrt{2/3} = 11.431$. We are not aware of any additional experiments on Ir to pressures comparable to those of [5]. However, subsequent theoretical studies based on *ab initio* approaches failed to confirm the existence of a transformation of fcc-Ir into another solid structure [9, 10]. Specifically, in [9] all possible atomic-layer arrangements for a 14-layer hex cell were considered and their T=0 enthalpies were compared to that of fcc-Ir as functions of atomic volume. The enthalpies of these different 14-layer structures form a family of quasi-parallel curves (figure 3 of ref. [9]; only sixty such distinct curves exist, out of a total of $\sim 2^{14}$, because of a high level of degeneracy [9]) such that the enthalpy differences are virtually independent of volume, yet all of these curves remain higher and never cross the fcc one. Hence, no transition from fcc-Ir can be inferred based on thermodynamic considerations. However, according to [9], the enthalpy difference between fcc and the most stable of the sixty 14-layer structures is only 12 meV/atom, or ~ 140 K; such a small difference can be easily overcome by contribution from the corresponding entropy term. Thus, at least some of the hex structures considered in [9] should be expected to become thermodynamically more stable than fcc with increasing T.

In the present work we determine the melting curve of Ir to ~ 600 GPa using the Z method, which we briefly describe in the following section. Our Z method calculations are carried

out using the quantum molecular dynamics (QMD) code VASP (Vienna Ab initio Simulation Package), which is based on density functional theory (DFT). We use the generalized gradient approximation (GGA) with the Perdew-Burke-Ernzerhof (PBE) exchange-correlation functional. We model Ir using the electron core-valence representation $[^{54}\mathrm{Xe}\ 4f^{14}]\,5d^7\,6s^2$, i.e. we assign the 9 outermost electrons of Ir to the valence. The valence electrons are represented with a plane-wave basis set with a cutoff energy of 370 eV, while the core electrons are represented by projector augmented-wave (PAW) pseudopotentials.

We first calculated the T=0 isotherm of fcc-Ir. This was done by performing a short QMD run and extracting the corresponding value of P. We used a $5 \times 5 \times 5$ (500-atom) supercell with a single Γ-point. With such a large supercell, full energy convergence (to $\lesssim$ 1 meV/atom) is already achieved, which was verified by performing short runs with $2 \times 2 \times 2$ and $3 \times 3 \times 3$ k-point meshes and comparing their output with that of the 500-atom run with a single Γ-point.

Our results on the T=0 isotherm are shown in figure 2. We note that each of the papers [5, 11, 12] that discuss Ir EOS data uses the 3rd-order Birch-Murnaghan (BM) EOS $P(\rho) = \frac{3}{2} B_0 \left((\rho/\rho_0)^{7/3} - (\rho/\rho_0)^{5/3} \right) \left[1 + \frac{3}{4}(B_0' - 4) \left((\rho/\rho_0)^{2/3} - 1 \right) \right]$, where B_0 and B_0' are the values of the bulk modulus and its pressure derivative at the reference point $\rho = \rho_0$. Since the P=0 values of the density of Ir at T=0 and 300 K differ by $\sim 0.4\%$ (22.65 vs. 22.56 g/cc [1]), and T=300 K introduces a negligibly small thermal pressure correction, the T=0 and T=300 K isotherms can be described by the same values of B_0 and B_0'. Consequently, we can compare room-T isotherm data to our T=0 isotherm as determined from QMD. This comparison is shown in figure 2. The experimental results from two groups, each of which accessed $P \sim 65$ GPa, were presented as BM fits with different choices for B_0 and B_0': $B_0 = 306$ GPa and $B_0' = 6.8$ and $B_0 = 354$ GPa and $B_0' = 4.0$ from [5] (the former set results from fitting with both B_0 and B_0' as free parameters, while the latter from fitting with $B_0' = 4.0$ kept fixed), and $B_0 = 383$ GPa and $B_0' = 3.1$ from [11]. Another set of parameters, $B_0 = 340$ and $B_0' = 4.8$ comes from theoretical modeling [12]. It is seen that although excellent agreement of the QMD points with the available experimental data (up to $\rho \sim 26$ g/cc) is found for each of the (B_0, B_0') sets, it is the 3rd-order BM isotherm with $B_0' = 5$ that best fits the QMD data at densities above the experimental range.

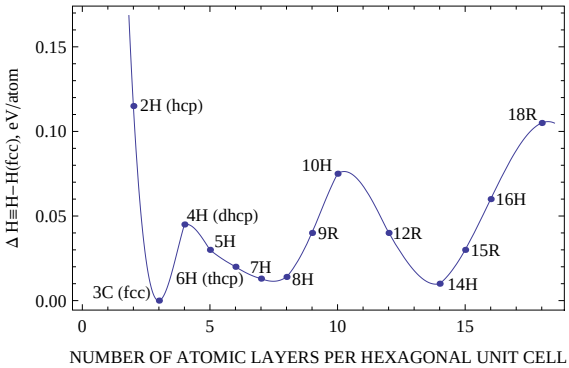

Figure 3. Differences between the T=0 enthalpies of hex structures of Ir and that of fcc-Ir as a function of the number of atomic layers per unit hex cell, at a fixed unit cell volume.

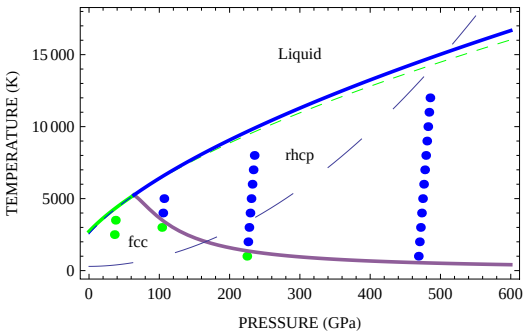

Figure 4. Phase diagram of Ir obtained from the Z methodology: fcc-Ir melting curve (green line), liquid Ir solidified into solid fcc (green bullets), 9R-Ir melting curve (blue line), liquid Ir solidified into solid rhcp (blue bullets), and the (tentative) fcc-rhcp solid-solid phase boundary (violet).

We then turned to hex structures of Ir. We calculated the T=0 enthalpies of different hex structures of Ir having the number of atoms per unit cell from 2 (hcp) to 18 (18R). This was

done by optimizing the value of c/a, i.e. determining the c/a that minimizes the energy, at a fixed volume of a hex supercell, and then performing a short QMD run and extracting the corresponding value of P. We used supercells with the number of atoms from 540 (for $6 \times 6 \times 1$ 15R) to 686 (for both $7 \times 7 \times 2$ 7H and $7 \times 7 \times 1$ 14H) with a single Γ-point. With such large supercells, just like for fcc-Ir, full energy convergence (to $\lesssim$ 1 meV/atom) is already achieved, which allowed us to resolve the enthalpy differences to high accuracy. We found out that all the hex structures of Ir have the values of c/a equal to the ideal ones to within 1%, so that basically $c/a = N\sqrt{2/3}$, where N is the number of atoms per unit cell, for all the unit cell volumes considered (P from 0 to $\sim$ 900 GPa). The hex enthalpies form a system of quasi-parallel curves similar to that shown in figure 3 of ref. [9]. Figure 3 shows different hex enthalpies (including that of fcc-Ir as 3C hex structure) as a function of the number of atoms or, equivalently, the number of atomic layers, per hex unit cell at some fixed unit cell volume (since the enthalpy curves are quasi-parallel, their differences do not depend on volume, thus for any other fixed unit cell volume the plot will look similar to that in figure 3). In figure 3, only the structures having the lowest enthalpy among those with the same number of layers per unit cell are shown, in each case that there are more than one such structure (for $N \geq 6$). Specifically, for the hexagonal structures listed below, points in figure 3 indicate the following (periodic) stacking sequences, 2H (hcp): AB, 3C (fcc): ABC, 4H (double-hcp, or dhcp): ABAC, 5H: ABCAC, 6H (triple-hcp, or thcp): ABCACB, 7H: ABCABAC, 8H: ABACBABC, 9R (α-Sm): ACABABCBC, 10H: ABACBACABC, 12R: ABABCACABCBC, 14H: ABACBCBACABCBC, 15R: ABABACACACBCBCB, 18R: ABACACBCBACABABCBC.

The plot clearly exhibits two distinct minima, for 7H and 8H, and for 14H the enthalpy of which is the closest one to that of fcc-Ir: the 14H-fcc enthalpy difference is 11 meV/atom, in agreement with [9]. Since none of the hex structures becomes more stable than fcc at T=0 (or T=300 K, according to the Ir phase diagram from Section 3), we offer the following explanation for the appearance of the 14-layer superstructure in experiments by Cerenius and Dubrovinsky. It is not clear from [5] how the hydrostaticity of the pressurized Ir was controlled (whether or not a pressure medium was used, etc.) It is quite possible that in their experiments nonhydrostatic stresses were present under the action of which fcc-Ir loses its thermodynamic stability and the hex structure that is energetically the closest one to fcc-Ir gets thermodynamically stabilized. Such a structure is 14H, with 14 atomic layers per unit cell, just like the one found in ref. [5].

2. Z method applied to the melting curve of Ir

Now we switch to the calculation of the melting curves of different solid structures of Ir using the Z method. The Z method was developed to calculate melting curves using first-principles based software, specifically VASP. The Z method was introduced for the first time in our paper on the *ab initio* melting curve of Mo [13]. The method has since been applied to the study of a large number of melting curves of different materials, and comparisons with experimental data on Pb, Ta, Fe and Pt at ESRF show good agreement [14]. In contrast to previous melting curve calculations based on the Z method, in our recent work on Os [15], the method was utilized as closely as possible to the original concept, but at the expense of an extensive suite of QMD simulations. Specifically, we directly observe melting in the computational cell, and then determine the corresponding melting temperature (T_m) and pressure (P_m) (at a given density); see [15] for more detail. Earlier on, T_m and P_m would be determined from bracketing the true melting point by the highest solid (P_s, T_s) and the lowest liquid (P_l, T_l) states on the Z-shaped isochore, and using $(P_m, T_m) \approx (\,(P_s + P_l)/2,\ (T_s + T_l)/2\,)$. Here we use the same idea of directly observing melting and directly calculating T_m and P_m for the melting curve of Ir. In the case of Ir, it is important to note that, if a material has more than one thermodynamically stable crystal structure, the Z method yields the solid-liquid equilibrium boundaries of those structures.

The phase having the highest solid-liquid equilibrium T over some pressure range is the most stable, thus the physical melting curve, including triple points, is the envelope of the solid-liquid equilibrium boundaries.

Here we applied this strategy to the study of the melting curve of Ir. We calculated the melting curves of the following 8 solid structures: fcc, hcp, dhcp, 7H, 8H, 9R, 14H, and 15R. We used the same supercells as for the T=0 enthalpy calculation described above. We simulated 4 melting points for each of the 4 structures fcc, hcp, 9R and 14H, and then, after these 4 melting curves were obtained, we simulated 2 melting points for each of the remaining 4 structures, dhcp, 7H, 8H and 15R, to see if they lie close to any of those 4 curves. At a given density we performed a sequence of very long runs, each up to 25000 time steps or 25 ps, with initial Ts separated by relatively small increments of 375 K. We performed 13 such runs for each of the 24 melting points on the 8 melting curves; that is, our simulations covered a range of initial T of 4500 K in each case. We carried out a total of 312 runs which, with an average of ~ 17500 time steps per run, amounted to a total of ~ 5.5 million time steps of our melting simulations.

The melting curve of *fcc*-Ir, as the best fit to the corresponding four QMD melting points, is described by (T_m in K, P in GPa) $T_m^{\rm fcc}(P) = 2719\,(1 + P/31.2)^{0.59}$. The melting curves of hcp, 14H and 15R are close or slightly below the fcc one. However, the melting curves of dhcp, 7H, 8H and 9R are all close to each other and cross that of fcc; in other words, another solid phase becomes thermodynamically more stable than *fcc*-Ir at high PT conditions. We chose 9R to be the prototype solid structure at high PT; its melting curve, as the best fit to the corresponding four QMD melting points, is described by $T_m^{\rm 9R}(P) = 2553\,(1 + P/27.5)^{0.60}$. The fcc and 9R melting curves cross each other at (P, T) = (64, 5250), the fcc-9R-liquid triple point. Both melting curves are shown in figure 4.

Since for a number of solid structures of Ir the solid-liquid equilibrium boundaries (melting curves) are indistinguishable within mutual error bars, these structures have very close free energies. Consequently, the most stable structure cannot be determined using the Z method, and an alternative approach is needed.

3. Inverse Z method applied to the phase diagram of Ir

To cope with this difficulty, and to locate the solid-solid phase boundary in Ir, we use the inverse Z method introduced in our earlier work [14] where it was applied to the study of the phase diagrams of Pt and Ta; see [14] for more detail. The method consists in solidifying the initially liquid state into a final solid structure at a given fixed T. The subsequent identification of the crystal structure of the final state can be done by means of a number of techniques: (i) comparison of radial distribution functions (RDFs); (ii) comparison of X-ray diffraction patterns in reciprocal momentum space; (iii) geometric structure analysis (coordination number, angles between interatomic bonds, etc.). Two different final-state crystal structures at (P_1, T_1) and (P_2, T_2) then bracket the corresponding solid-solid phase boundary.

Here we applied the inverse Z method to locate the solid-solid boundary in Ir. We used a computational cell of 686 atoms prepared by melting a $7 \times 7 \times 7$ solid bcc supercell which should avoid bias towards solidifying either into fcc or any of the hex structures. We carried out NVT simulations using the Nosé-Hoover thermostat with a timestep of 1 fs. Complete solidification typically required from 15 to 25 ps, or $15000 - 25000$ timesteps, which is comparable with the duration of a typical direct-Z NVE run; the 25 inverse-Z runs (figure 4) contributed to a total of ~ 0.5 million time steps, in addition to ~ 5.5 million from direct-Z melting simulations.

We found that Ir solidifies into fcc below the violet line in figure 4, while above this line it solidifies into a hex structure. The line is described by the equation (T in K, P in GPa) $T(P) = 10500/(1+(P/64)^{1.5})$. The Ir principal Hugoniot described by [16] $T(P) = 293+0.087653\,P^{1.9332}$ crosses this line at (P, T) = (166.5, 2020), the Hugoniot transition point, such that the transition pressure of 166.5 GPa is consistent with 160 ± 20 GPa from SWD.

The RDFs did not allow us to discriminate between different hex structures: *hcp*, *dhcp*, *thcp*, $9R$, etc. Upon fast quenching of the hex structures to low T, where RDFs are more discriminating, we observed all of the above four hex structures, and perhaps some other hex structures as well. Hence, the inverse Z method indicates that there may be a number of energetically competitive hex structures of Ir at high PT. Our results indicate that structures with different stacking sequences are energetically very close. Hence, the energy cost of forming a stacking fault between two such structures is virtually zero. Consequently, the actual layer stacking could be non-periodic and, in principle, random. A random-stacking hex close-packed (*rhcp*) structure was first introduced for hard-sphere colloids [17], and has since been the subject of literature discussions [18, 19]. In general, when different stacking sequences become energetically degenerate, that is, the energy difference between any two such structures is $\sim 1-10$ meV per atom, or $\sim 10-100$ K, then in the resulting structure any two adjacent layers can occur with equal probability.

We are not yet aware of any direct reference to elements with a *rhcp* structure, except for our own suggestion that Pt may be such an element (having *rhcp* as its high PT phase [14]). In view of the fact that a *rhcp* phase may have been discovered experimentally in Au above 250 GPa by Dubrovinsky *et al.* [20] (see [14] for more detail), all the three third-row fcc noble metals Ir, Pt and Au become good candidates for being *rhcp* elements.

4. Conclusions

To conclude, we have applied the Z methodology, a novel technique for the computation of both melting curves and solid-solid phase boundaries, to the study of the phase diagram of Ir, and our results compare favorably with the existing experimental data. This study demonstrates that the Z methodology is a powerful utility for the calculation of phase diagrams. With the knowledge of the T=0 solid-solid transition points from the cold free-energy calculations, and of the solid-solid-liquid triple points from the direct Z method, complete solid-solid phase boundaries can be constructed, as both the previous examples of Pt and Ta [14] and the present example of Ir clearly demonstrate. We have offered the following explanation for the 14-layer hex structure observed by Cerenius and Dubrovinsky: because of possible nonhydrostaticity in their experiments, fcc-Ir loses its stability and converts into the energetically closest hex structure, 14H, with the periodic layer stacking ABACBCBACABCBC.

References

[1] Arblaster J W 2010 *Platinum Metals Rev.* **54** 93-102
[2] http://www.periodictable.com/Properties/A/ShearModulus.v.html
[3] Arblaster J W 2013 *Platinum Metals Rev.* **57** 177-85
[4] Zil'bershteyn V A and Estrin E I 1968 *Fiz. Metal. Metalloved.* **28** 369-70 and references therein
[5] Cerenius Y and Dubrovinsky L 2000 *J. Alloys Compounds* **306** 26-9
[6] Shock R N and Johnson K 1971 *Fiz. Metal. Metalloved.* **31** 1100-1
[7] http://www.ihed.ras.ru/rusbank/
[8] Greeff C W 2005 *Model. Simul. Mater. Sci. Eng.* **13** 1015-27
[9] Grussendorff S, Chetty N and Dreysse H 2003 *J. Phys. Cond. Mat.* **15** 4127-34
[10] Cawkwell M J *et al.* 2006 *Phys. Rev. B* **73** 064104; Fang H *et al.* 2010 *Physica B* **405** 732-7
[11] Cynn H, Klepeis J E, Yoo C-S, and Young D A 2002 *Phys. Rev. Lett.* **88** 135701
[12] Kuchhal P and Dass N 2003 *Pramana* **61** 753-7; Kapoor K, Kumar A and Dass N 2014 *ibid.* **82** 549-61
[13] Belonoshko A B *et al.* 2008 *Phys. Rev. Lett.* **100** 135701
[14] Burakovsky L *et al.* 2014 *J. Phys. Conf. Ser.* **500** 162001 and references therein
[15] Burakovsky L, Burakovsky N and Preston D L 2015 *Phys. Rev. B* **92** 174105
[16] Kinslow R, editor 1970 *High-Velocity Impact Phenomena* Academic Press, New York and London, p. 547
[17] Auer S and Frenkel D 2001 *Nature* **409** 1020-3
[18] Dolbnya I P, Petukhov A V, Aarts D G, Vroege G J and Lekkerkerker H N W 2005 *Europhys. Lett.* **72** 962-8
[19] Byelov D V *et al.* 2010 *Phase Transitions* **83** 107-14
[20] Dubrovinsky L *et al.* 2007 *Phys. Rev. Lett.* **98** 045503